Original Article

Electroacupuncture of the Baihui and Shenting acupoints for vascular dementia in rats through the miR-81/IL-16/PSD-95 pathway

Chunmei Ma[1#], Ying Zhou[1#], Wei Yi[2], Xianxi Zhou[3], Wenping Guo[1], Xiaowu Xu[1], Jing Luo[1], Ziwei Luo[1], Aijun Liu[3], Dongfeng Chen[1]

[1]Department of Anatomy, School of Basic Medical Sciences, Guangzhou University of Chinese Medicine, Guangzhou, China; [2]Medical College of Acupuncture, Moxibustion and Rehabilitation, Guangzhou University of Chinese Medicine, Guangzhou, China; [3]Center for Experimental Teaching, School of Basic Medical Sciences, Guangzhou University of Chinese Medicine, Guangzhou, China

Contributions: (I) Conception and design: D Chen, A Liu, C Ma; (II) Administrative support: D Chen, A Liu; (III) Provision of study materials or patients: C Ma, Y Zhou; (IV) Collection and assembly of data: W Yi, X Zhou, W Guo, Y Zhou; (V) Data analysis and interpretation: C Ma, J Luo, Z Luo, X Xu; (VI) Manuscript writing: All authors; (VII) Final approval of manuscript: All authors.

[#]These authors contributed equally to this work.

Correspondence to: Dongfeng Chen. Department of Anatomy, Guangzhou University of Chinese Medicine, 232 East Waihuan Road, Guangzhou Higher Education Mega Center, Panyu District, Guangzhou 510006, China. Email: cdf27212@21cn.com; Aijun Liu. Center for Experimental Teaching, School of Basic Medical Sciences, Guangzhou University of Chinese Medicine, 232 East Waihuan Road, Guangzhou Higher Education Mega Center, Panyu District, Guangzhou 510006, China. Email: aijunliu@gzucm.edu.cn.

Background: There is currently no effective treatment for vascular dementia (VaD). Scalp electroacupuncture (EA) has served clinically as an alternative treatment for VaD, but its mechanism is still unclear. In this study, we investigated the effect of EA at the Baihui (GV 20) and Shenting (GV 24) acupoints on spatial learning and memory ability, and the expression level of *microRNA-81* (*miR-81*), *interleukin-16* (*IL-16*), and postsynaptic density protein-95 (PSD-95) in the frontal cortex of VaD rats.

Methods: Male Sprague-Dawley rats were randomly divided into four groups, sham, VaD, non-acupuncture (non-AP) and EA group. The VaD model was established by permanent bilateral occlusion of the common carotid arteries. Morris Water Maze was used to assess the rats' spatial learning and memory. Immunochemistry (IHC), quantitative reverse transcription polymerase chain reaction (qRT-PCR), and western blot analysis were performed to detect the expression level of *miR-81*, *IL-16*, and PSD-95. Finally, luciferase assay was used to determine the effect of *miR-81* on *IL-16* expression in PC12 cells.

Results: The space exploration experiment of MWM showed the time and distance of the rat's activities around the platform were decreased in the EA group. Compared to the VaD and non-AP group, the number of terminal deoxynucleotidyl transferase-mediated dUDP nick-end labeling (TUNEL)-positive frontal cortical neurons was significantly decreased in EA group. The number of the PSD-95-positive cells and the *miR-81* expression level in the frontal cortical in the EA group was dramatically increased in comparison with the other groups. In the PC12 cell validation experiment, *IL-16* expression level was reduced under the condition of the *miR-81* mimic treatment, while increased in the *miR-81* inhibitor group. The PSD-95 protein level was up-regulated in the small interfering (*si*)*RNA-IL16* group compared to the *NC-IL16* groups with or without oxygen/glucose deprivation/reperfusion (OGD/R) conditions ($P<0.05$). However, this was abolished by *miR-81* mimic.

Conclusions: In VaD rats, EA may improve spatial learning and memory through miR-81/IL-16/PSD-95 pathway.

Keywords: Baihui acupoint (GV 20); electroacupuncture (EA); *miR-81*; Shenting acupoint (GV 24); vascular dementia (VaD)

Submitted Mar 23, 2022. Accepted for publication May 13, 2022.
doi: 10.21037/atm-22-2068
View this article at: https://dx.doi.org/10.21037/atm-22-2068

Introduction

Vascular dementia (VaD) refers to a cognitive syndrome due to brain tissue injury from a series of cerebrovascular factors, and results in severe, irreversible damage to the central nervous system. Among the various forms of dementia, VaD has an incidence rate that is widely considered to be second only to that of Alzheimer's disease (AD) (1). A study shows that the pathogenesis of VaD is complex, which is caused by the damage of localized larger vessels in brain or cumulative cerebral smaller vascular diseases (2). Therefore, vascular injury is the key of neuronal loss and synaptic disintegration. The resulting autophagy, apoptosis and inflammation induce to the occurrence and development of cerebrovascular conditions and cognitive impairment (3). Markers of processes, such as autophagy, apoptosis, endothelial activation, inflammation, and oxidative stress, are enhanced in the endothelial cells (4). Importantly, these processes can lead to neuronal death, which in turn causes cognitive and behavioral disorders.

Acupuncture is one of the most central components of traditional Chinese medicine (TCM). Multiple studies have reported that acupuncture affects microRNA (miRNA) expression in the brains of animal models for hypoxia/ischemia, effectively improves learning and memory, and reduces neuronal apoptosis (5-7). Electroacupuncture increases neuronal survival and induces dendritic regeneration in the ischemic penumbra of cerebral artery occlusion/reperfusion (MCAO/R) rats through brain-derived neurotrophic factor/TrkB (BDNF/TrkB) pathway, thereby enhancing neuronal plasticity and functional recovery (8). Additionally, electroacupuncture trigeminal nerve stimulation (EA/TNS) could induce serotonin and norepinephrine expression in the brainstem, then enhance BDNF secretion, subsequently modulate neurotransmitter receptors and PSD-95 expression, and ultimately regulate synaptic plasticity.

The miRNAs/miRs, are non-coding, small nucleic acids which regulate different cellular pathways. They are emerging as new biomarkers and targets of nervous system diseases. Treatments based on miRNA include miRNA mimics and inhibitors, which decrease and increase the expression of their target genes, respectively (9). Neuritis in 2-vessel occlusion (2-VO) rats can be modulated by acupuncture inhibition of *miR-93*-mediated toll-like receptor 4 (TLR4) signaling pathways (7). The expression of *miR-137* is significantly decreased in rats with chronic cerebral hypoperfusion and significantly upregulated after electroacupuncture (EA). In rats with reduced brain perfusion, EA can inhibit neuronal apoptosis, improve learning disorders, and alleviate brain injury. Moreover, EA may also regulate the *miR-137/NOX4* axis (10). The mechanism for increased LIM kinase-1 induced by EA may involve *miR-134* located in the hippocampal CA1 region, where it enhances synapse-dendrite plasticity during the recovery phase of ischemic stroke through the negative regulation of *LIM kinase-1* (11). Notably, *miR-150* knockout was shown to significantly reduce cognitive disorders in rats with VaD and inhibit neuronal apoptosis in their brain tissue (12).

In recent years, scalp acupuncture has played major roles in increasing blood supply to the cerebral cortex, thereby increasing the neuronal metabolic rate, as well as promoting synapse formation between brain cells (13). Scalp acupuncture is popular in Asia due to its simple application, safety, and efficacy. Acupuncture is an economical TCM therapy with few side effects; it has been used for thousands of years in Asia for numerous diseases, including the rehabilitation stage following stroke. Based on the principles of ancient Chinese acupuncture, EA involves the electrical stimulation of acupoints with acupuncture needles. It is a simple, convenient, and economical procedure that has been widely applied to cognitive disorders caused by cerebral ischemia (14,15). The scalp is an important region with respect to EA for improving neurological function in patients with ischemic stroke (16,17); however, the mechanism underlying the effects of EA have not been fully elucidated.

Postsynaptic density protein-95 (PSD-95) is an important postsynaptic protein in excitatory neurons in synapse formation, synaptic plasticity, and synaptic targeting of α-amino-3-hydroxy-5-methyl-4-isoxazole propionic acid receptors; they mediate most of the excitatory transmissions in the central nervous system. Furthermore, PSD-95 belongs to PSD protein family and exerts functions in neural synapse formation and stability through regulating

neural synaptic strength and plasticity (18). As mentioned previously, miRNAs are small molecules containing approximately 23 non-coding RNA that can downregulate the expression of target genes through post-transcriptional gene silencing. It has been shown that miRNAs are involved in the pathogenic mechanism of nervous disease and may explain the potential effects of acupuncture (19). However, studies linking the functional mechanisms of miRNAs and the effects of acupuncture are lacking. In this study, we have found three kinds of miRNA in the frontal cortex of 2-VO rats of the electroacupuncture group which are significantly higher than those of the model group. *MiR-81* is the most significant one which this study chooses. The purpose of this study is to explore whether acupuncture can reduce neuronal injury and cognitive impairment by increasing miR-81 mediated IL-16/PSD-95 pathway. We present the following article in accordance with the ARRIVE reporting checklist (available at https://atm.amegroups.com/article/view/10.21037/atm-22-2068/rc).

Methods

Animals and materials

Male specific-pathogen-free Sprague-Dawley (SD) rats were purchased from the Southern Medical University Experimental Animal Center (license number: SCXK [Yue] 2016-0041; Guangdong, China). All the rats were approximately 8 weeks old, weighed 220–280 g, and were acclimated for 1 week before the experiments. The rats were housed (n=4 per cage) at 25±1 ℃ with a relative humidity of 50–70% under a 12-hour light/dark cycle (lights on at 7:00 am), and all rats had free access to food and water. The study was approved by the Institutional Animal Care and Use Committee of the Guangzhou University of Chinese Medicine (No. 20181023004), and was conducted in compliance with the Guide for the Care and Use of Laboratory Animals, 8th edition. A protocol was prepared before the study without registration.

Experimental protocol: Experiment 1

To observe cognitive function in rats with VaD, and the changes in frontal lobe neurons and their postsynaptic scaffold proteins, chronic ischemia was established in 42 4-week-old rats using the 2-VO model while 12 rats were used as the sham group. There were two 2-VO-rats died during the operation and four died within 24 hours after that. After 7 days of environmental adaptation, 48 rats were assigned into four groups (12 rats/group) according to randomisation list, namely: sham group, VaD group, non-acupuncture (non-AP) group, and EA group. The Morris water maze (MWM) test was administered on day 14 after treatment. We then randomly selected 6 rats from each group, applied anesthesia, and immediately perfused them through the aorta with −4 ℃ normal saline and 4% paraformaldehyde solution. Brain tissue was collected, embedded in paraffin, and prepared into 4 μm-thick slices for hematoxylin and eosin staining, terminal deoxynucleotidyl transferase-mediated dUDP nick-end labeling (TUNEL) apoptosis testing, and immunohistochemical (IHC) staining.

Experimental protocol: Experiment 2

To verify whether *miR-81* inhibits *IL-16* expression in the frontal cortex, 6 rats from each group were anesthetized and immediately euthanized 24 hours after the MWM test. The remaining 6 rats in each group were anesthetized using an intraperitoneal injection (0.15 mL/100 g body weight) of 100 mg/kg ketamine and 10 mg/kg xylazine. The rats were then sacrificed, brain tissue was immediately removed and stored at −80 ℃, then total RNA was subsequently extracted. The expression level of *miR-81* was detected among the 4 groups, and *miR-81* mimics and inhibitors were used to interfere with *IL-16* expression in PC12 cells. Additionally, a luciferase reporter assay was performed to confirm the *miR-81* mimics and inhibitors.

Establishment of a VaD model

Rats were anesthetized by the intraperitoneal injection with 100 mg/kg of ketamine and 10 mg/kg xylazine, then the 2-VO model was established by the following steps. First, the rat was placed on the operating table with its ventral side up and upper limbs fixed. The skin from the neck to the chest was disinfected locally twice with iodophor and disinfected with 75% alcohol for deiodination. Second, an approximately 1 cm long incision was made from the middle of the neck to the chest. Third, a glass needle was used to carefully separate subcutaneous tissue and deep muscles, to expose the common carotid artery on both sides between the muscles and avoid pulling and damaging the vagus nerve. Fourth, an embedded silk thread was placed under the common carotid artery with a glass needle, and bilateral ligation was performed to cause permanent blockade. Fifth, the wound was sutured and clamped with 2–3 sterile wound clips. Finally, the residual blood was wiped from the wound

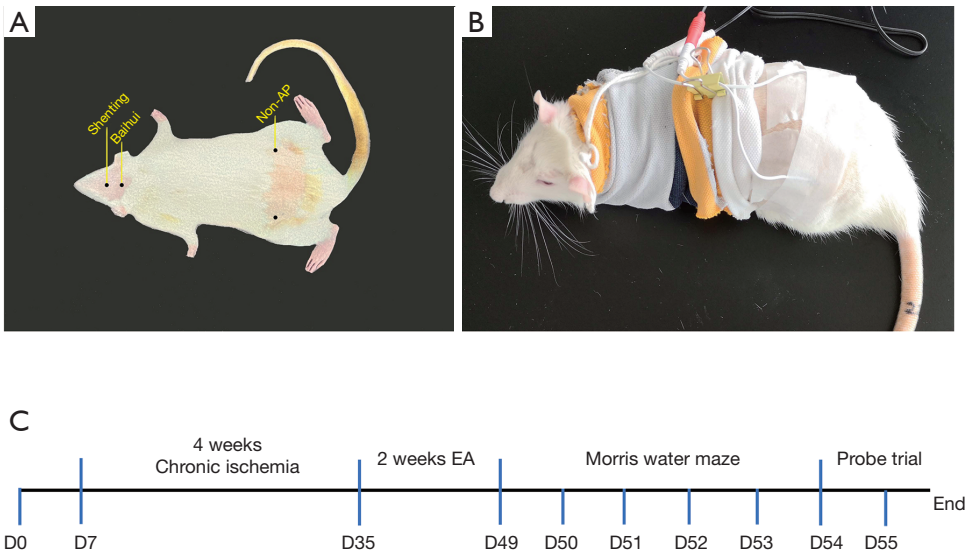

Figure 1 Electroacupuncture rats exhibit recovery of memory (n=12/group). (A) Localization of acupoints and non-acupoints used by electroacupuncture; (B) a self-made rat cover; (C) timeline of animal experiments. EA, electroacupuncture.

with iodophor, and erythromycin eye ointment was applied with a medical cotton swab to disinfect the incision and surrounding skin to prevent infection of the wound. After the operation, the rat was kept warm with an incandescent lamp for 6 hours. The bilateral common carotid arteries were separated and permanently ligated, inducing sustained hypoxic ischemia in the brain tissue. This causes progressive hypoxic-ischemic injury to the neurons and microcirculation in brain regions sensitive to injury (e.g., cerebral cortex, hippocampus), thereby simulating the pathological environment of VaD. In the sham group, arterial ligation was not performed but all the other operations were the same as those performed for the VaD group.

EA

On day 29 after model establishment, EA was performed on the Baihui and Shenting acupoints in the EA group. The specific acupuncture sites are shown in *Figure 1*. The EA was applied by stainless steel needles (7 mm in length and 0.18 mm in diameter; Suzhou Acupuncture and Moxibustion Appliance Co., Ltd., Suzhou, China) and an EA apparatus (Huatuo-SDZ-II, Suzhou Medical Appliance Co., Ltd., Suzhou, China). The Baihui acupoint was selected as the intersection of the line between the ears and midline of the head and the needle inserted 15° obliquely to a depth of 2 mm. The Shenting acupoint was selected as the anterior midline at the anterior intersection with the coronal suture and the needle was inserted into the skin to a depth of 4-5 mm and an angle of 15° relative to the tip of the nose. In the non-AP group, the acupuncture sites were situated posteriorly, 1 cm above each iliac joint (*Figure 1A*). The rats were immobilized using a self-made rat cover that exposed only the head to prevent them from struggling excessively during the intervention, which can affect the treatment (*Figure 1B*) (20). The rats were kept conscious, and the EA apparatus was connected and secured with a bandage. Then, a longitudinal wave was selected and a current of 3.0 mA was applied with a frequency of 2 Hz. This entire procedure was performed daily for 30 minutes per session. The EA and non-AP groups underwent EA for 14 days (at different sites), whereas the VaD and sham groups were immobilized for 30 minutes per day, and no EA was performed.

MWM

To assess spatial learning and memory, we performed the MWM test 24 hours after the final EA treatment (Guangzhou Feidi Biology Science and Technology Co., Ltd., Guangzhou, China). We used a black circular pool that measured 180 cm in diameter and 60 cm in height, which was divided into 4 quadrants (northeast, northwest, southeast, and southwest). The pool was filled to a depth

of 30 cm with water at a temperature of 22±2 ℃. During the experiment, a black opaque safety platform, measuring 29 cm in height and 20 cm in diameter, was placed in a random quadrant, 25–30 cm from the edge of the pool. The platform position remained unchanged, and the water was kept clean throughout the experiment, which was performed every morning on days 1–5 post-treatment. Each rat was considered to have safely found the platform if it found the platform within 90 seconds and remained standing on the platform for >3 seconds. If the rat did not find the platform successfully within 90 seconds, a tool was used to guide it towards the platform and keep it there for 20 seconds to help it remember the platform's location. The maximum escape latency was recorded as 90 seconds. Each day, the rats were released one after the other into each of the 4 quadrants once, and the escape latency was recorded. The experimental process was automatically recorded and analyzed using a water maze video analysis system. Space exploration experiments were performed on post-treatment day 6. The safety platform was removed, but the platform was unchanged in the recording system. We recorded and observed the number of times the rats crossed the initial platform area within 90 seconds as well as their search strategies. The rats were dried at the end of each experiment.

Reverse transcription quantitative polymerase chain reaction analysis

We extracted total RNA using a total RNA extraction kit (EZBioscience, Roseville, MN, USA), and the concentration and purity of extracted RNA were measured by ultraviolet spectrometry. We used the Prime Script reverse transcription kit (Takara Biotechnology Co., Ltd., Dalian, China) for reverse transcription. The thermal cycling conditions were set 37 ℃ for 15 minutes and 85 ℃ for 4 seconds. For *miR-81*, a specific reverse transcription primer was used (5'-GTCGTATCCAGTGCAGGGTCCGAGGTATTCGCACTGGATACGACCCTCAG-3'), whereas a random primer was used for U6 reverse transcription. We used the SYBR premix EX Taq kit (Takara Biotechnology Co., Ltd., China) for quantitative polymerase chain reaction (qPCR). Relative quantification of gene expression was performed using the CFX96 real-time PCR system. The thermal cycling conditions were as follows: 95 ℃ for 30 seconds, followed by 40 cycles of denaturation at 95 ℃ for 5 seconds, annealing at 55 ℃ for 30 seconds, elongation at 72 ℃ for 1 minute, and finally, 55 ℃ for 5 seconds. The following primers were used for *miR-81* qPCR: forward primer 5'-CGTTGGGGATGGTAGGGTCT-3', and reverse primer 5'-AGTGCAGGGTCCGAGGTATT-3'. We purchased U6 qPCR primers from Sangon Biotechnology Co., Ltd. (Shanghai, China; No. MQP-0101). The *miR-81* expression level was determined by using the $2^{-\Delta\Delta Cq}$ method. We used U6 as the internal sham for miRNA quantitation. The procedure was repeated three times.

Bioinformatics prediction of miR-81 target genes

The target gene of *Rattus norvegicus miR-81* was predicted using TargetScan (version 7.2; www.targetscan.org/mmu_71). We performed a gene function analysis using Venn diagrams and the Database for Annotation, Visualization, and Integrated Discovery (DAVID) bioinformatics database version 6.8. The target genes of *miR-81* were verified by a luciferase reporter gene analysis. The procedure was repeated three times.

Histopathological observation of hematoxylin-eosin staining

The frontal cortex and hippocampus were dehydrated, embedded in paraffin, sliced into sections of 4 μm, and finally stained with hematoxylin and eosin (HE) using an HE staining kit (Beijing Solarbio Science & Technology Co., Ltd., Guangzhou, China). We used an optical microscope (Leica dMI400, Leica Microsystems Shanghai trading Co., Ltd., Shanghai, China) for imaging. The procedure was repeated six times.

TUNEL staining

Paraffin sections of the frontal cortex were dried and routinely deparaffinized and dehydrated using xylene and an ethanol gradient and TUNEL kit (Shanghai Beyotime Biotechnology Co., Ltd., Shanghai, China). Drops of the corresponding reagents were added, and 50 μL TUNEL detection solution was added to each slide. The slides were incubated at 37 ℃ for 60 minutes in the dark, mounted with anti-fluorescence quenching mounting solution containing 4', 6-diamidino-2-phenylindole (DAPI), and observed using a fluorescence microscope [Nikon Instruments (Shanghai) Co., Ltd, Shanghai, China]. The procedure was repeated six times.

IHC staining

We incubated the paraffin sections of the frontal cortex

with anti-PSD-95, a primary antibody (1:500; catalog no. 20665-1-AP; Proteintech; Stockport, UK) and a biotinylated secondary antibody at 37 ℃ for 20 minutes. Staining was examined using an optical microscope at 400× magnification. We observed 5 fields in each section for measurement of PSD-95 expression. We used an optical microscope (Leica dMI400, Leica Microsystems Shanghai trading Co., Ltd., China) for imaging. The procedure was repeated three times.

PC12 cell culture

It is common for PC12 (coming from rat pheochromocytoma) cells to be used in neurobiological research. We purchased PC12 cells (Procell Life Science & Technology Co. Ltd., Hyderabad, India) and incubated them at 37 ℃ with 5% CO_2. The primary reagents were Roswell Park Memorial Institute (RPMI) 1640 medium (Gibco, Thermo Fisher Scientific, Inc., Waltham, MA, USA), 10% fetal bovine serum (FBS; Gibco, Thermo Fisher Scientific, Inc., USA), and 1% penicillin/streptomycin (Gibco, Thermo Fisher Scientific, Inc., USA). The medium was changed every 2–3 days, and the PC12 cells were cultured in a 6-well cell culture plate at a density of 5×10^5 cells/well.

Luciferase reporter analysis

We cultured the PC12 cells in a 24-well cell culture plate at a density of 1×10^5 and transfected them with *miR-81* mimic, *miR-81* inhibitor, *miR-81* mimic-NC (negative control), or *miR-81* inhibitor-NC (Guangzhou RiboBio Co., Ltd, Guangzhou, China). Lipofectamine 2000 (Gibco, ThermoFisher Scientific, Inc., USA) was used to co-transfect the *pLUC-IL-16-wild* type 3'-untranslated region (UTR) or p*LUC-IL-16-mutant* 3'-UTR (Nanjing Tsingke Biotechnology Co., Ltd, Nanjing, China). Regarding the *pLUC-IL-16* cloning vector, TargetScan software version 7.2 was used to predict the miRNA target sites based on the experimental protocol, which were inserted adjacent to the Renilla luciferase fragment. The *miR-81* mimic, and miRNA mimic negative sham transfected into PC12 cells was 50 nM. In addition, the *miR-81* inhibitor and miRNA inhibitor negative sham was used at 100 nM. A total 200 ng of plasmid was transfected into cells in each well. After 48 hours, the PC12 cells were lysed, and the dual luciferase reporter quantitative analysis kit was used for detection. The procedure was repeated three times.

Transfection of PC12 cells with miR-81 mimic, miR-81 inhibitor, and their corresponding negative shams or siRNA-IL-16

For transfection, PC12 cells were seeded in a 6-well cell culture plate at a density of 9×10^5 and grown to a confluence of 60–80%. We transfected *miR-81* mimic (5'-UUGGGGAUGGUAGGGUCUCUGAGG-3' and 5'-UCAGAGCCCUACCAUCCCCAAUU-3'), *miR-81* mimic-NC (5'-UUCUCCGAACGUGCUAGGUTT-3'), *miR-81* inhibitor (5'-CCUCAGAGACCCUAC CAUCCCCAA-3'), and *miR-81* inhibitor-NC (5'-UUGUACUACACAAAAGUACUG-3') as per the manufacturer's instructions. We transfected small interfering (*si)RNA (siR)-IL-16-001* (5'-CCAGGUUUCAAGAUGCCAATT-3') and *siR-IL-16-002* (5'-UUGGCAUCUUGAAACCUGGTT-3') using Lipofectamine 2000 (Gibco, Thermo Fisher Scientific, Inc., USA). The mimic, mimic-NC, and siRNA at 50 nM and inhibitor and inhibitor-NC at 100 nM were applied in cell tests. Cells were lysed in radioimmunoprecipitation assay (RIPA) buffer (Sigma-Aldrich, St. Louis, MO, USA) 48 hours after transfection for reverse transcription (RT)-qPCR analysis. The procedure was repeated three times.

Western blot analysis

Cells were homogenized in RIPA buffer containing protease inhibitor and phosphatase inhibitor, then kept on ice for 30 minutes, and centrifuged at 12,000 rpm for 20 minutes at 4 ℃. The supernatant was collected, and total protein was quantified using the bicinchoninic acid (BCA) Protein Assay (Thermo Fisher, USA). Proteins (30 μg per well) were separated by 10% sodium dodecyl sulfate-polyacrylamide gel electrophoresis (SDS-PAGE) and transferred onto polyvinylidene difluoride (PVDF) membranes (Millipore, Burlington, MA, USA). Membranes were blocked with 5% bovine serum albumin (BSA; Roche, Mannheim, Germany) and incubated with primary antibodies [PSD-95, 1:2,000, Abcam (Cambridge, MA, USA), USA; β-actin, 1:5,000, Abcam, USA] overnight at 4 ℃. After incubation with secondary antibodies (anti-mouse, 1:5,000, Abcam, USA) for 1 hour at room temperature, the membranes were developed with electrochemiluminescence (ECL) solution (Millipore, USA) and exposed to an X-ray film. For quantification, the mean intensity of bands was measured using the Image J software (National Institutes of Health, Bethesda, MD, USA). The procedure

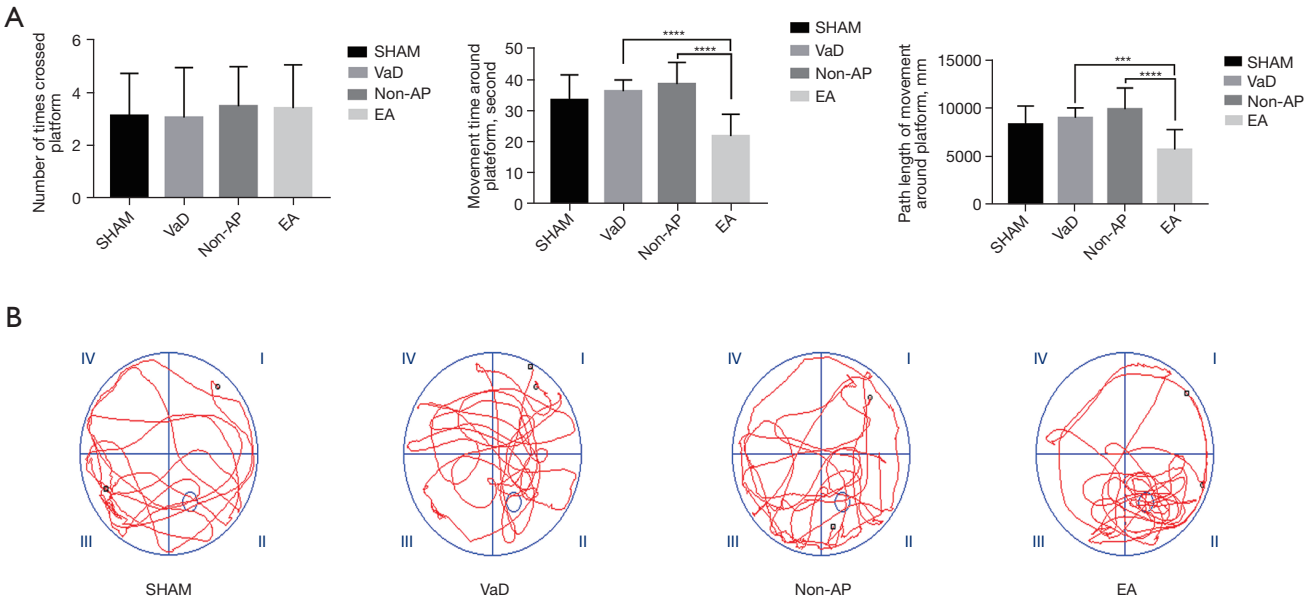

Figure 2 Electroacupuncture rats exhibit recovery of memory (n=12/group). (A) Times to cross the platform, path length of movement around the platform, and duration of movement around platform in the four groups during a Morris water maze test, compared with the EA group; (B) the moving trails of rats in the probe trial. VaD, vascular dementia; AP, acupuncture; EA, electroacupuncture. Statistical significance between both groups was defined as ***P<0.001; ****P<0.0001.

was repeated three times.

Statistical analysis

All data were presented as the means ± standard deviations (SD) of triplicated independent experiments. The data were analyzed using SPSS 23.0 software (IBM Corp., Armonk, NY, USA) and GraphPad Prism7 (version 7.0; GraphPad Software, Inc., San Diego, CA, USA). The t test was used for comparison between two groups, and comparisons among multiple groups were using a one-way analysis of variance (ANOVA) followed by Tukey's multiple comparisons test for post-hoc analysis. If the quality characteristic value was not in the Gauss distribution, Kruskal-Wallis analysis was carried out. A P value <0.05 was considered to indicate a statistically significant difference.

Results

EA improves memory of 2-VO rats

At 4weeks after 2-VO (*Figure 1C*), the rats in the EA group, that underwent EA for 2 weeks, showed recovery of memory. In the MWM test, the average escape latency of the sham, non-AP, and EA groups in the directional navigation experiment decreased to varying degrees with an increase in the number of trials, but no significant difference was observed among the four groups (P>0.05). From the space exploration experiment, there was no significant difference among the groups regarding the number of times the rats crossed the platform site within 90 seconds, but the time and distance of the activities around the platform were significantly decreased in the EA group (*Figure 2A*). The swim path maps showed that each group of rats passed through the safety platform site in the space exploration experiment and exhibited different search strategies (*Figure 2B*).

EA improves frontal cortical and hippocampal neuronal injury and apoptosis in rats with 2-VO

After EA, the histopathological changes in the frontal cortex and hippocampus were observed by HE staining. The number of frontal cortical neurons in the sham group was large, and they had an intact structure, abundant cytoplasm, and clearly visible nuclei. In the VaD group, we observed a loss of frontal lobe neurons, shrunken nuclei, darker staining of neurons, and unclear neuronal structure (*Figure 3A*). In the EA group, abnormalities in the frontal cortical neurons were reduced, the

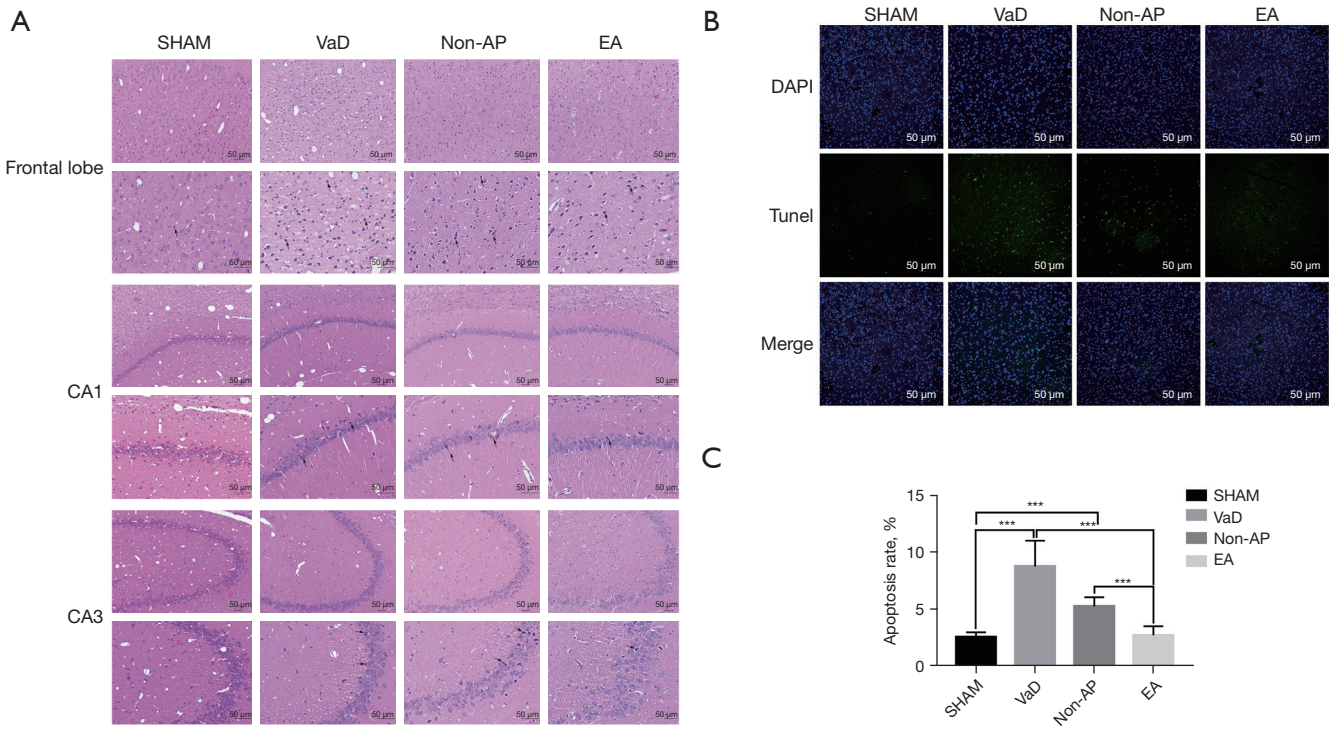

Figure 3 Histopathological changed in the frontal lobe, and hippocampal CA1 and CA3 regions (n=6/group). (A) Representative images of morphological changed in cerebral cortex, the hippocampal CA1 and CA3 regions in the sham, VaD, non-AP, and EA groups (n=6/group), 2 weeks after EA staining (HE staining; magnification ×200 and ×400). Scale bar, 50 μm. Nuclear pyknosis was indicated with black arrow. (B) TUNEL staining for apoptosis detection. Expression of apoptotic factors in the cortices of rats among all four groups. Scale bar, 50 μm. (C) Apoptosis rate in the cortex of rats. Data were shown as mean ± SD values, and statistical significance between both groups was defined as ***P<0.001. VaD, vascular dementia; AP, acupuncture; EA, electroacupuncture; HE, hematoxylin and eosin; TUNEL, terminal deoxynucleotidyl transferase-mediated dUDP nick-end labeling; CA1, cornu ammonis 1; CA3, cornu ammonis 3.

number of neurons was larger, and the pathological damage was milder. In addition, TUNEL staining was used to detect apoptotic neurons. In the EA group, the number of TUNEL-positive frontal cortical neurons was decreased compared to that in the VaD and non-AP groups, but there was no significant difference between the non-AP and VaD groups in this regard (*Figure 3B,3C*). These results indicate that EA can improve frontal cortical neuronal injury in rats with VaD. Notably, however, the improvement in the hippocampus was not significant (*Figure 3*).

EA increases the number of PSD-95-positive granules and miR-81 expression in rats with 2-VO

The IHC products of PSD-95 comprise small, brown particles distributed in the frontal cortex and hippocampus. The number and grayscale values of the PSD-95-positive cells in the frontal cortical neurons in the EA group were significantly increased compared to those in the VaD and non-AP groups (*Figure 4A,4B*). However, the change in the hippocampus was not significant. Furthermore, we identified a new miRNA to help elucidate the mechanism of EA for VaD. We performed RT-qPCR analysis to determine the content of miR-81 in the cortex of VaD rats (n=6/group). The results showed that *miR-81* expression level in the frontal cortex of the EA group was more than that in the VaD and non-AP groups. There were no significant differences in hippocampal *miR-81* expression among the groups (*Figure 4C*). These results indicate that EA can increase PSD-95 expression in frontal cortical neurons, and that *miR-81* is associated with VaD induced by chronic ischemia as well as EA treatment. They also highlight the differential expression of *miR-81* in the frontal cortex not hippocampus of rats with VaD.

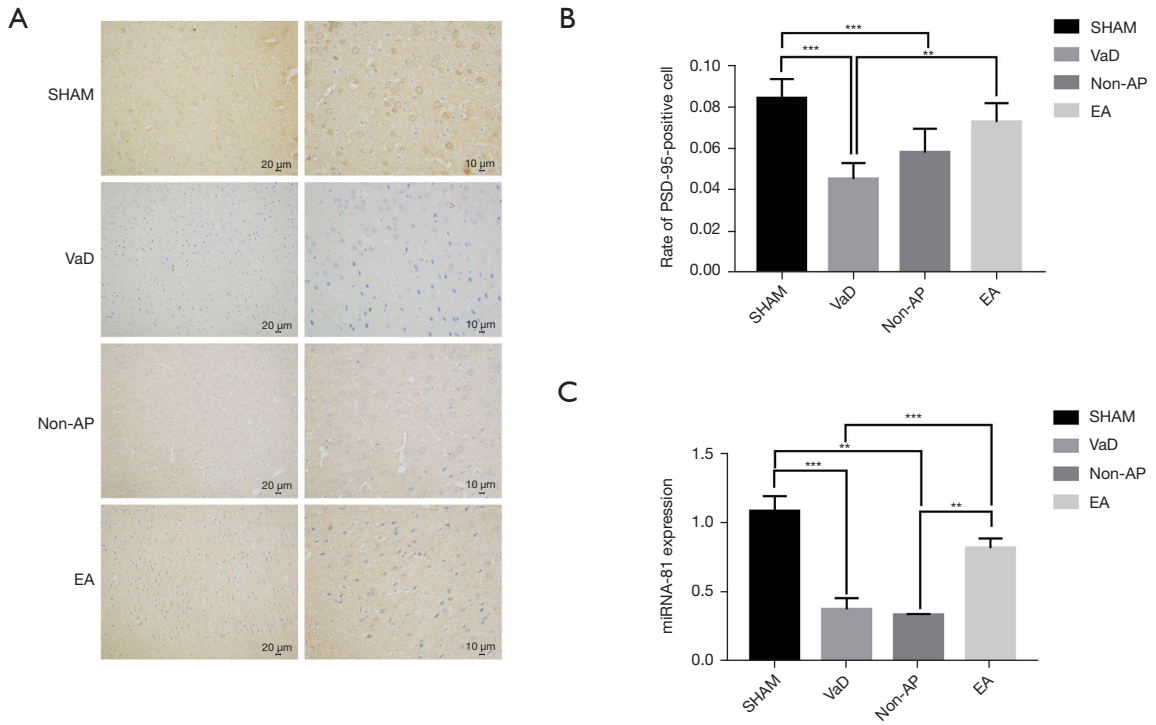

Figure 4 The expression of PSD-95 was detected by immunohistochemical staining (n=6/group). (A) Immunohistochemical staining of paraffin sections was used to observe the expression of PSD-95 (n=6/group). Scale bar, 10 μm and 20 μm. (B) The number and grayscale values of PSD-95-positive cells in the EA group were significantly increased compared to the VaD group. Statistical significance between both groups is defined as **P<0.01. ***P<0.001. (C) Expression of *miR-81* in cortex of EA group was significantly higher than that of the VaD and non-AP groups. **P<0.01, ***P<0.001. There was no significant difference in *miR-81* expression in hippocampal tissue among the groups. VaD, vascular dementia; AP, acupuncture; EA, electroacupuncture; ANOVA, analysis of variance.

IL-16 is a potential target of miR-81

Binding sites in the *miR-81* sequence (5'-GUCAGUG-3') and the *IL-16* gene sequence (5'-CAGUCAC-3') were predicted via bioinformatics analysis (*Figure 5A*). To evaluate the direct effects of *miR-81* on *IL-16* gene expression, we constructed a dual luciferase reporter carrying the *miR-81* target site in pLUC-IL-16 (*Figure 5B*). The data indicated that the *miR-81* mimic decreased the luciferase activity of *IL-16*. Contrastingly, the *miR-81* mimic did not decrease activity of luciferase while the *miR-81* seed sequence of the *IL-16* 3'UTR was mutated (*Figure 5C*). We used RT-qPCR to determine whether miRNA mimics and inhibitors were successfully transfected into PC12 cells (n=3/group). The results showed that *miR-81* expression was significantly higher in the mimic group than in the mimic control group, and that *miR-81* expression in the inhibitor group was significantly lower than that in the inhibitor control group (*Figure 5D*), indicating that the transfection was successful.

To further assess the relationship between *miR-81* and *IL-16*, PC12 cells were divided into 4 groups: *miR-81* mimic, *miR-81* mimic-NC, *miR-81* inhibitor, and *miR-81* inhibitor-NC. After transfecting PC12 cells with *miR-81* mimic, *miR-81* mimic-NC, *miR-81* inhibitor, and *miR-81* inhibitor-NC, the relative expression of *IL-16* mRNA was measured using RT-qPCR. Overall, *IL-16* expression was decreased in the mimic group compared to the mimic-NC group and increased in the inhibitor group compared to the inhibitor-NC group (*Figure 5E*). These results indicate that *miR-81* directly regulates *IL-16*.

Interleukin-16 mediates the effect of miR-81 on regulation of PSD-95

To determine whether IL-16 mediates the effect of *miR-81* on regulation of PSD-95, *IL-16* expression was silenced in PC12 cells subjected to oxygen glucose deprivation/

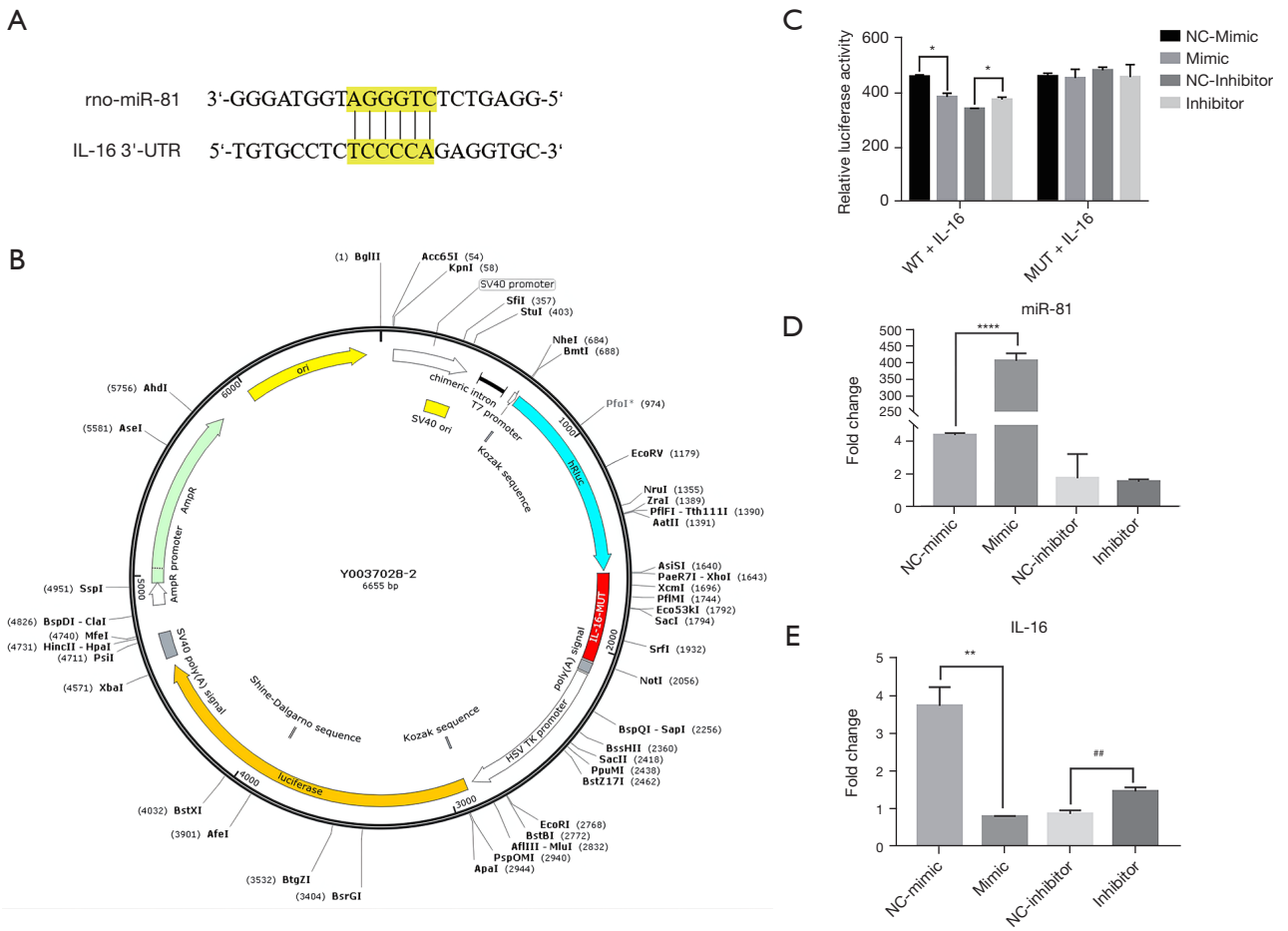

Figure 5 The *IL-16* 3'-UTR is the specific target of miR-81. (A) Binding sites of miR-81 were present in the 3'-UTR of *IL-16*. TargetScan was used to identify the target sites. (B) Construction profile of the psiCHECK *IL-16* plasmid. The binding sequence in the *IL-16* 3'-UTR was replaced in the psiCHECK-IL-16 MUT plasmid. (C) The relative luciferase activity of psiCHECK-IL-16 was reduced by *miR-81*. We transfected PC12 cells with the psiCHECK-2-IL-16 vector (200 ng), *miR-81* mimic (100 nM), or *miR-81* mimic-NC (100 nM) for 48 h using Lipofectamine 2000. *P<0.05 *vs. miR-81* NC + psiCHECK-IL-16 group. Data were presented as the mean ± standard error of the mean. Untransfected cells were used as the sham group. (D) The expression of *IL-16* mRNA was reduced by *miR-81* in PC12 cells. We transfected PC12 cells with *miR-81* mimic (100 nM), *miR-81* mimic-NC (100 nM), *miR-81* inhibitor, and *miR-81* inhibitor-NC for 48 h using Lipofectamine 2000. ****P<0.0001. Data were presented as the mean ± standard error of the mean. (E) The expression of IL-16 mRNA was reduced in PC12 cells due to miR-81. **P<0.01 *vs.* mimic-NC, ##P<0.01 *vs.* inhibitor-NC. *IL-16*, interleukin-16; UTR, untranslated region; miR, microRNA; NC, negative control; WT, wild type; MUT, mutant; mRNA, messenger RNA.

reperfusion (OGD/R) injury and followed by *miR-81* mimic/inhibitor treatment. Western blot analysis revealed PSD-95 protein levels were increased in the *si-IL16* group compared to the NC-IL16 group in or not in OGD/R conditions (P<0.05) (*Figure 6*), but the overall levels of both were reduced in OGD/R conditions (P<0.01). However, this was relieved by *miR-81* mimic (P<0.05 *vs. NC-IL16* + NC-mimic + NC-inhibitor + OGD group), but in the absence of *IL-16*, PSD-95 was downregulated in cells treated with *miR-81* mimic (i.e., NC-IL16 + mimic + NC-inhibitor + OGD *vs. Si-IL16* + mimic + NC-inhibitor + OGD; P<0.05). These results indicate that *IL-16* is required for the effects of *miR-81* for the regulation of PSD-95 in OGD/R injury.

Discussion

Currently, it is difficult to treat and achieve a cure in VaD patients as no specific clinical treatment has been

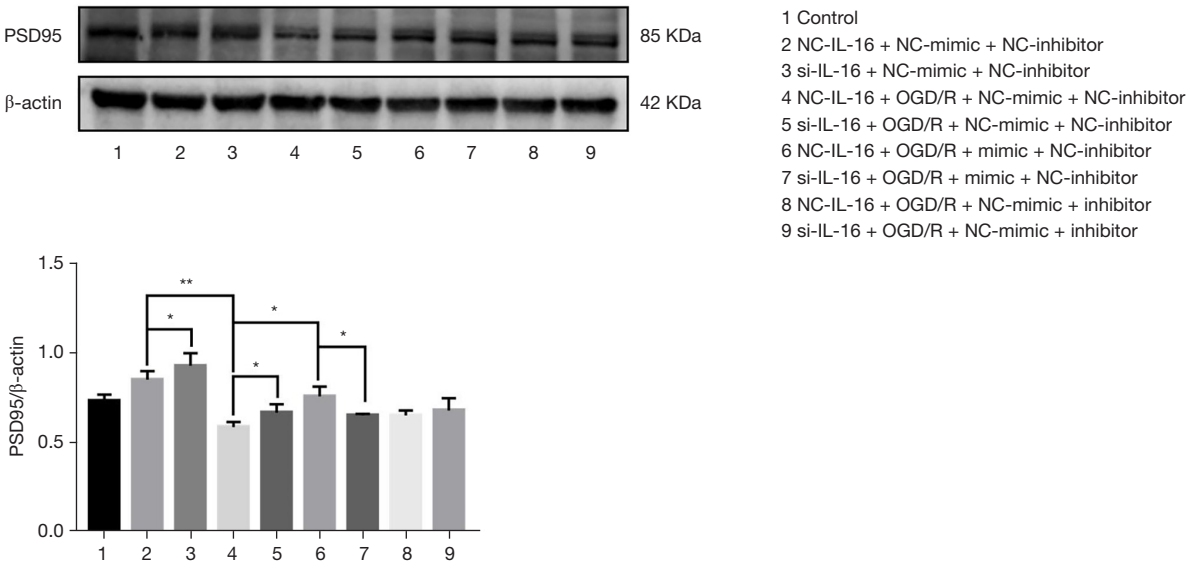

Figure 6 Western blot analysis of the role of *IL-16* in *miR-81* regulating PSD-95 expression. PC12 cells were co-transfected for 48 h with si-*IL-16* (50 nM), the NC siRNA (50 nM) and *miR-81* mimic (50 nM), *miR-81* inhibitor (100 nM), *miR-81* mimic-NC (50 nM), *miR-81* inhibitor-NC (100 nM) using Lipofectamine 2000. *P<0.05; **P<0.01. Data are presented as the mean ± standard error of the mean. NC, negative control; siRNA, small interfering RNA.

established. However, Chinese acupuncture is widely used throughout Asia, particularly in China, due to its safety, simple operation, and good curative efficacy. Early acupuncture intervention has major clinical significance with respect to VaD. In TCM, EA is an important method for the treatment of VaD that was developed based on the combination of theories of traditional acupuncture theory and scalp projection in cortical function in Western medicine, but its mechanism of action is relatively complex and not well understood. Based on TCM theory, VaD belongs to the category of "stupidity" and "forgetfulness" and results from the imbalance of Yin with Yang or the disorder of Qi or blood. The Du meridian, known as the Governing Vessel (GV), is one of the 8 extraordinary channels and is regarded as the sea of the Yang channels. Among the 8 meridians, Yin-Yang and deficiency-excess distribute the 2 radical nutritive and defensive energies (or fundamental Yin and Yang in both quality and quantity) to the meridians and organs. The head is located at the top of the body, into which flow certain meridians (or channels) and the Qi and blood from the organs (Zangfu). Baihui (GV 20) and Shenting (GV 24) are important acupoints of Du meridian, which have been proved to improve post-stroke dysfunction (21,22). According to the theory of traditional Chinese medicine, Du Meridian is related to the regulation of many neural functions and is used to treat brain diseases (14). Baihui is located on the apex place of the head where all the yang meridians meet and shenting is the intersection of Qi and blood. The two acupoints are associated with the regulation of several brain functions and are used to treat brain disorders (23,24). Although there are some common adverse events, such as bleeding, pain at the acupuncture site and fainting during acupuncture, both of them can clear the mind, lift the spirits (25). Clinically, Baihui and Shenting are principle acupoints which are often selected to improve the impaired functions such as motor control and cognition of patients after stroke (26).

Our previous study found that the expression of proteins of certain miRNAs, such as *miR-134-5p*, reduced cortical neurons and synaptic proteins by inhibiting Foxp2 and downstream syn1 protein, thus aggravating cognitive impairment of VaD rats (5). Recent clinical studies have shown that miRNAs can be used as potential biomarkers for various neurological diseases, for example, the downregulation of miR-132 in CSF can be applied to diagnose post-stroke cognitive impairment (PSCI) (27), while the miR-222 level in the VaD group was significantly upregulated compared with both the control and AD group (28). Because the main way of laboratory research is intraventricular administration, in view of the complexity of

its clinical operation, it has not been reported to be applied to patients (29). A few miRNAs play a regulatory role in the pathogenic mechanism of VaD. Moreover, regulating the levels of these miRNAs represents a potential intervention against stroke in model animals undergoing EA. To further investigate the mechanism of EA in improving VaD and alleviating brain tissue damage, we identified a new miRNA through administration of EA to the Baihui and Shenting acupoints in rats with VaD. Specifically, in the EA group, *miR-81* was significantly increased in the frontal cortical neuronal tissue compared to the VaD group. Target gene prediction and luciferase reporter gene analysis showed that *miR-81* is a direct target of *IL-16*, and that the memory of rats who underwent EA improved. The level of *IL-16* was increased in ischemic cerebrovascular dementia and AD cases, confirming that the immune system plays an extremely important role in the development and progression of neurodegenerative diseases (30).

Destruction of the blood-brain barrier is associated with a cognitive decline and may involve inflammatory mechanisms based on serum IL-16, vascular endothelial growth factor-D, and IL-15 (31). A study reports that 7 inflammatory/immune molecules, including IL-16, in the cerebrospinal fluid of patients with AD, neuroinflammation, and vascular injury show good performance characteristics with respect to assays for technical performance. These are potential biomarkers associated with neurovascular injury that can be reliably measured in the cerebrospinal fluid and show good biotemporal stability (32). Notably, PSD-95 is a postsynaptic marker that is widely distributed in all nerve terminals and serves as an important protein marker of regeneration and remodeling. It is used to quantify the number of axon terminals and reflects the presence, density, and strength of synapses (33,34). Many previous studies have reported that the hippocampal expression of synaptophysin and PSD-95 is decreased in AD and VaD (35,36). It has also been shown that acupuncture can upregulate PSD-95 expression (37) and promote the repair of synaptic structural damage, thereby improving learning and memory in the vascular cognitive impairment mouse model (38,39). Furthermore, in 5XFAD mice, EA was shown to improve working memory and synaptic plasticity, reduce neuroinflammation, and reduce ultrastructural degradation of synapses through the upregulation of synaptophysin and PSD-95 (40). Pre-treatment of EA reduces the production of reactive oxygen species and *NOX4* expression, which may be related to restoration of the blood-brain barrier function (41).

In this study, acupuncture stimulation of the Baihui and Shenting acupoints stimulated the production of miR-81 in the frontal cortex of rats with VaD, downregulated its target IL-16, and reduced neuronal apoptosis in the frontal cortex, thereby promoting the expression of the postsynaptic membrane scaffold protein PSD-95 and improved the learning and memory of rats with VaD, and these were proved in PC12 cells under OGD/R conditions. In conclusion, this study is only aimed at animal experiments and miR-81 may become a potential therapeutic target for vascular dementia. It will be more meaningful to increase clinical research in the future. However, the relationship between *miR-81*, *IL-16*, and PSD-95 needs to be assessed further via future experiments.

Acknowledgments

Funding: This work was sponsored by the National Natural Science Foundation of China (grant No. 81673770).

Footnote

Reporting Checklist: The authors have completed the ARRIVE reporting checklist. Available at https://atm.amegroups.com/article/view/10.21037/atm-22-2068/rc

Data Sharing Statement: Available at https://atm.amegroups.com/article/view/10.21037/atm-22-2068/dss

Conflicts of Interest: All authors have completed the ICMJE uniform disclosure form (available at https://atm.amegroups.com/article/view/10.21037/atm-22-2068/coif). The authors have no conflicts of interest to declare.

Ethical Statement: The authors are accountable for all aspects of the work in ensuring that questions related to the accuracy or integrity of any part of the work are appropriately investigated and resolved. The study was approved by the Institutional Animal Care and Use Committee of the Guangzhou University of Chinese Medicine (No. 20181023004), and was conducted in compliance with the Guide for the Care and Use of Laboratory Animals, 8th edition.

References

1. Korczyn AD, Vakhapova V, Grinberg LT. Vascular dementia. J Neurol Sci 2012;322:2-10.
2. Bir SC, Khan MW, Javalkar V, et al. Emerging Concepts in Vascular Dementia: A Review. J Stroke Cerebrovasc Dis 2021;30:105864.
3. Wang XX, Zhang B, Xia R, et al. Inflammation, apoptosis and autophagy as critical players in vascular dementia. Eur Rev Med Pharmacol Sci 2020;24:9601-14.
4. Rouhl RP, Damoiseaux JG, Lodder J, et al. Vascular inflammation in cerebral small vessel disease. Neurobiol Aging 2012;33:1800-6.
5. Liu X, Zhang R, Wu Z, et al. miR-134-5p/Foxp2/Syn1 is involved in cognitive impairment in an early vascular dementia rat model. Int J Mol Med 2019;44:1729-40.
6. Lai XS, Wang L. Effect of Electroacupuncture on Learning and Memory and Apoptosis of Hippocampal Neurons in Vascular Dementia Rats. Acupuncture Research 2003;28:245-50.
7. Wang L, Yang JW, Lin LT, et al. Acupuncture Attenuates Inflammation in Microglia of Vascular Dementia Rats by Inhibiting miR-93-Mediated TLR4/MyD88/NF-κB Signaling Pathway. Oxid Med Cell Longev 2020;2020:8253904.
8. Li SS, Hua XY, Zheng MX, et al. Electroacupuncture treatment improves motor function and neurological outcomes after cerebral ischemia/reperfusion injury. Neural Regen Res 2022;17:1545-55.
9. Sun P, Liu DZ, Jickling GC, et al. MicroRNA-based therapeutics in central nervous system injuries. J Cereb Blood Flow Metab 2018;38:1125-48.
10. Bi X, Feng Y, Wu Z, et al. Electroacupuncture Attenuates Cognitive Impairment in Rat Model of Chronic Cerebral Hypoperfusion via miR-137/NOX4 Axis. Evid Based Complement Alternat Med 2021;2021:8842022.
11. Liu W, Wu J, Huang J, et al. Electroacupuncture Regulates Hippocampal Synaptic Plasticity via miR-134-Mediated LIMK1 Function in Rats with Ischemic Stroke. Neural Plast 2017;2017:9545646.
12. Wei C, Xu X, Zhu H, et al. Promotive role of microRNA-150 in hippocampal neurons apoptosis in vascular dementia model rats. Mol Med Rep 2021;23:257.
13. Li J, Man Q, Wang W, et al. Scalp acupuncture for patients with vascular dementia: A protocol for systematic review and meta-analysis of randomized controlled trails. Medicine (Baltimore) 2020;99:e22798.
14. Li X, Guo F, Zhang Q, et al. Electroacupuncture decreases cognitive impairment and promotes neurogenesis in the APP/PS1 transgenic mice. BMC Complement Altern Med 2014;14:37.
15. Liu W, Wang X, Zheng Y, et al. Electroacupuncture inhibits inflammatory injury by targeting the miR-9-mediated NF-κB signaling pathway following ischemic stroke. Mol Med Rep 2016;13:1618-26.
16. Hsing WT, Imamura M, Weaver K, et al. Clinical effects of scalp electrical acupuncture in stroke: a sham-controlled randomized clinical trial. J Altern Complement Med 2012;18:341-6.
17. Wang X, Zhang Q, Cui B, et al. Scalp-cluster acupuncture with electrical stimulation can improve motor and living ability in convalescent patients with post-stroke hemiplegia. J Tradit Chin Med 2018;38:452-6.
18. El-Husseini AE, Schnell E, Chetkovich DM, et al. PSD-95 involvement in maturation of excitatory synapses. Science 2000;290:1364-8.
19. Ko JH, Kim SN. MicroRNA in Acupuncture Studies: Does Small RNA Shed Light on the Biological Mechanism of Acupuncture? Evid Based Complement Alternat Med 2019;2019:3051472.
20. Cao Z, Liu A, Yan X, et al. Making and using a simple holder for acupuncture in rats. Journal of Gansu University of Chinese Medicine 2018;35:24-6.
21. Lin R, Chen J, Li X, et al. Electroacupuncture at the Baihui acupoint alleviates cognitive impairment and exerts neuroprotective effects by modulating the expression and processing of brain-derived neurotrophic factor in APP/PS1 transgenic mice. Mol Med Rep 2016;13:1611-7.
22. Feng X, Yang S, Liu J, et al. Electroacupuncture ameliorates cognitive impairment through inhibition of NF-κB-mediated neuronal cell apoptosis in cerebral ischemia-reperfusion injured rats. Mol Med Rep 2013;7:1516-22.
23. Wang WW, Xie CL, Lu L, et al. A systematic review and meta-analysis of Baihui (GV20)-based scalp acupuncture in experimental ischemic stroke. Sci Rep 2014;4:3981.
24. Lin R, Wu Y, Tao J, et al. Electroacupuncture improves cognitive function through Rho GTPases and enhances dendritic spine plasticity in rats with cerebral ischemia-reperfusion. Mol Med Rep 2016;13:2655-60.
25. Chuang CM, Hsieh CL, Li TC, et al. Acupuncture

stimulation at Baihui acupoint reduced cerebral infarct and increased dopamine levels in chronic cerebral hypoperfusion and ischemia-reperfusion injured sprague-dawley rats. Am J Chin Med 2007;35:779-91.
26. Zhan J, Pan R, Guo Y, et al. Acupuncture at Baihui(GV 20) and Shenting(GV 24) combined with basic treatment and regular rehabilitation for post-stroke cognitive impairment:a randomized controlled trial. Zhongguo Zhen Jiu 2016;36:803-6.
27. Zhang M, Bian Z. Alzheimer's Disease and microRNA-132: A Widespread Pathological Factor and Potential Therapeutic Target. Front Neurosci 2021;15:687973.
28. Marchegiani F, Matacchione G, Ramini D, et al. Diagnostic performance of new and classic CSF biomarkers in age-related dementias. Aging (Albany NY) 2019;11:2420-9.
29. Yuan M, Bi X. Therapeutic and Diagnostic Potential of microRNAs in Vascular Cognitive Impairment. J Mol Neurosci 2020;70:1619-28.
30. Di Rosa M, Dell'Ombra N, Zambito AM, et al. Chitotriosidase and inflammatory mediator levels in Alzheimer's disease and cerebrovascular dementia. Eur J Neurosci 2006;23:2648-56.
31. Bowman GL, Dayon L, Kirkland R, et al. Blood-brain barrier breakdown, neuroinflammation, and cognitive decline in older adults. Alzheimers Dement 2018;14:1640-50.
32. Trombetta BA, Carlyle BC, Koenig AM, et al. The technical reliability and biotemporal stability of cerebrospinal fluid biomarkers for profiling multiple pathophysiologies in Alzheimer's disease. PLoS One 2018;13:e0193707.
33. Yu CC, Wang Y, Shen F, et al. High-frequency (50 Hz) electroacupuncture ameliorates cognitive impairment in rats with amyloid beta 1-42-induced Alzheimer's disease. Neural Regen Res 2018;13:1833-41.
34. Citri A, Malenka RC. Synaptic plasticity: multiple forms, functions, and mechanisms. Neuropsychopharmacology 2008;33:18-41.
35. Martin SB, Dowling AL, Lianekhammy J, et al. Synaptophysin and synaptojanin-1 in Down syndrome are differentially affected by Alzheimer's disease. J Alzheimers Dis 2014;42:767-75.
36. Dong J, Zhao J, Lin Y, et al. Exercise improves recognition memory and synaptic plasticity in the prefrontal cortex for rats modelling vascular dementia. Neurol Res 2018;40:68-77.
37. Yang G, Pei YN, Shao SJ, et al. Effects of electroacupuncture at "Baihui" and "Yongquan" on the levels of synaptic plasticity related proteins postsynaptic density-95 and synaptophysin in hippocampus of APP/PS1 mice. Zhen Ci Yan Jiu 2020;45:310-4.
38. Wang Y, Wang Q, Ren B, et al. "Olfactory Three-Needle" Enhances Spatial Learning and Memory Ability in SAMP8 Mice. Behav Neurol 2020;2020:2893289.
39. Xia WG, Zheng CJ, Zhang X, et al. Effects of "nourishing liver and kidney" acupuncture therapy on expression of brain derived neurotrophic factor and synaptophysin after cerebral ischemia reperfusion in rats. J Huazhong Univ Sci Technolog Med Sci 2017;37:271-8.
40. Cai M, Lee JH, Yang EJ. Electroacupuncture attenuates cognition impairment via anti-neuroinflammation in an Alzheimer's disease animal model. J Neuroinflammation 2019;16:264.
41. Jung YS, Lee SW, Park JH, et al. Electroacupuncture preconditioning reduces ROS generation with NOX4 down-regulation and ameliorates blood-brain barrier disruption after ischemic stroke. J Biomed Sci 2016;23:32.

(English Language Editor: J. Jones)

Cite this article as: Ma C, Zhou Y, Yi W, Zhou X, Guo W, Xu X, Luo J, Luo Z, Liu A, Chen D. Electroacupuncture of the Baihui and Shenting acupoints for vascular dementia in rats through the miR-81/IL-16/PSD-95 pathway. Ann Transl Med 2022;10(10):540. doi: 10.21037/atm-22-2068

